ELSEVIER

Journal of Organometallic Chemistry 661 (2002) 111–127

Journal of Organometallic Chemistry

www.elsevier.com/locate/jorganchem

Phosphane- and phosphorane *Janus Head* ligands in metal coordination

Frank Baier [a], Zhaofu Fei [a], Heinz Gornitzka [b], Alexander Murso [a], Stefan Neufeld [a], Matthias Pfeiffer [a], Ina Rüdenauer [a], Alexander Steiner [c], Thomas Stey [a], Dietmar Stalke [a,*]

[a] *Institut für Anorganische Chemie der Universität Würzburg, Am Hubland, D-97074 Würzburg, Germany*
[b] *Laboratoire Hétérochimie et Applique, Université Paul Sabatier 118, route de Narbonne, 31062 Toulouse, France*
[c] *Department of Chemistry, University of Liverpool, Crown Street, Liverpool L69 7ZD, UK*

Received 30 April 2002; accepted 15 July 2002

Dedicated to Professor Helmut Werner on the occasion of his retirement in recognition of his tremendous contributions to organometallic chemistry

Abstract

Our principal strategy to include the substituent periphery of phosphanides and phosphoranates in metal coordination is outlined. Rather than providing merely bulk or stereo information like in classical phosphane ligands to d-block metal centres the 2-pyridyl substituted species supply a second coordination site. Additional to the found σ/π coordination site selectivity these *Janus Head* ligands might serve as anionic staples in mixed Group 13/d-block metal complexes in homogeneous catalysis. The classical $NP(Ph_2)N^-$ chelating ligand is converted into a $NP(Py_2)N^-$ tripodal ligand. The pyridyl substitution has not only considerable impact on the metal coordination but also on the reactivity, emphasising the fact that this heteroaromatic substituent cannot simply be regarded as *eka*-phenyl. It facilitates double P–C bond cleavage and reduction of iminophosphoranes to phosphanamines in a one-pot reaction. Even P=N bond cleavage is observed. Several new routes to multidentate ligands in metal side-arm coordination were established.

Keywords: Alkali metals; Alkaline earth metals; Catalysis; P ligands; *Janus Head* ligands; N ligands

1. Introduction

A principal strategy in synthetic inorganic and organometallic chemistry is the employment of tailor made ligand systems to create metal complexes of specific nuclearity, coordination number, geometry, and reactivity. Typical functions of such ligands are to inhibit oligomerisation reactions, to stabilise the low valent form and/or the low oxidation state of the metal centre, and to model the shape of the complex periphery. These ligands need to provide significantly high flexibility since metal centres of soft and hard Lewis acidity require to be complexed each in the most suitable fashion. In addition to the capability to delocalize electron density, a multifunctional ligand should have a geometric adaptability as well, i.e. it should be variable enough to accommodate metal centres which are different in size within a moderate range. In terms of its sterical demand and cone angle the resulting chelating ligand should be comparable to the ubiquitous $C_5Me_5^-$ ligand. Those were the prerequisites we faced when working in the Würzburg research framework entitled 'Selective reactions of metal-activated molecules'. The substantial role of ligands at catalytically active d-block metal centres is obvious: especially phosphanes provide labile donor centres to release active sites. In addition, they supply sterical bulk to increase solubility and stereochemical information to be transferred to the products [1]. One of the most efficient co-catalysts are Group 13 organometallic moieties [2].

* Corresponding author. Tel.: +49-931-8884783; fax: +49-931-8884619
E-mail address: dstalke@chemie.uni-wuerzburg.de (D. Stalke).

0022-328X/02/$ - see front matter
PII: S0022-328X(02)01818-1

Methyl alumoxane (MAO) has become a key component in single site catalytical processes [3]. This article outlines our synergistic combination of two important concepts in ligand design to furnish catalytically improved moieties in Group 13 organometallics: heteroatomic chelation in coordination site selectivity and at heteroaromatic coordination [4] known e.g. from porphyrins. This new approach might raise the Group 13 organometallics from their current important but subordinate role as co-catalysts to outstanding catalysts on their own right [5].

The classic role of phosphane ligands at catalytic active d-block metal centres is exemplified in a variety of organometallic complexes studied in cooperation with Werner and coworkers [6]: apart from terminal monodentate phosphane ligands [6a] two phosphorus centres might be connected *via* a bridge variable in length [6c,6d]. The two connected donating atoms do not both have to be phosphorus. The hemilabile chelating ligands contain a P and As or Sb centre where the lower Lewis basicity of the heavier Group 15 element causes easier release of active sites at the metal (Chart 1a).

Chart 1. A classical chelating diphosphane (a) and the *Janus Head* ligand with coordinating periphery (b).

However, coordination of the metal in this phosphane and phosphane/arsane ligands is always reached via the Group 15 element while the organic substituents (namely phenyl) only provide the bulk. We aimed to design Group 15 element centred ligands which are able to employ their substituent periphery in metal coordination (Chart 1b). The implementation of additional coordinating sites divorced from the anionic centre would enhance the versatility of the ubiquitous phosphane ligands. Thus, the incorporation of the pyridyl substituents on the phosphorus centre in the place of the phenyl groups, alters and augments the coordination capability of the ligand system and leads to the concept of multi-dentate *Janus Head* ligands (Chart 2) [7].

In the di(pyridyl)phosphanides one face of the *Janus Head* is provided by the divalent P(III) centre while the two ring nitrogen atoms in the heteroaromatic substituents represent the second face (Chart 2a). The di(pyridyl)aminoiminophosphoranate anion has two potential chelating sites, firstly the $[N–P–N]^-$ skeleton, predominantly accommodating the negative charge, and secondly the two remote nitrogen atoms in the rings. Free rotation about the $P–C_{ipso}$ bond can easily bring

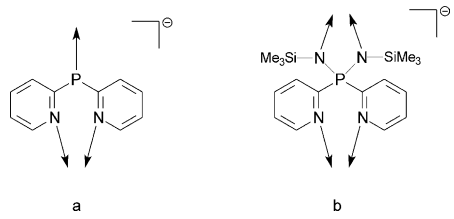

Chart 2. A phosphanide (a) and a phosphoranate (b) with two different coordination sites.

the pyridyl nitrogen atoms into the right position to coordinate metals of different radii. In addition, potential π-interaction of the heteroaromatic rings to the metal would stabilise the resulting complex (Chart 2b) [8].

Divalent P(III) compounds are established since the synthesis of the di(ketonato)phosphane **a** in Chart 3 [9,14]. The metallated species show different to most metal phosphanides no P–M contact. The substituents at the α-carbon atom might be varied as shown in **b** [10]. Remote chelating of the metal is not limited to oxygen atoms but may also be achieved by nitrogen atoms in the di(guanidinato)phosphanide **c** [11] or even by fluorine atoms in the di(fluorosilyl)phosphanides **d** [12]. Likewise the chelation is not restricted to lithium but can also be found to aluminium (**e** and **f**) [13,14]. However, none of the known species shows a donor atom in a heteroaromatic substituent. Therefore, we favoured the 2-pyridyl substituent (Py) to be connected to the Group 15 element.

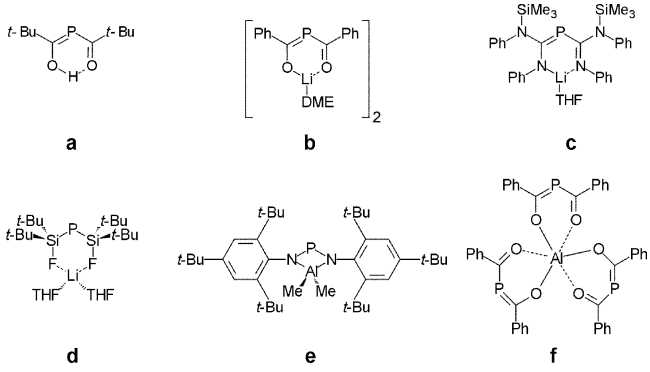

Chart 3. Known molecules with divalent phosphorus(III) centres without metal–phosphorus contact.

2. Pyridyl substituted phosphanes and phosphanides [5]

Tri(pyridyl)phosphane reacts with an equimolar amount of lithium metal in THF yielding deep crimson coloured solutions containing $[(THF)_2LiPy_2P]$ (**1**) and 2,2′-bipyridine in a 2:1 molar ratio (Eq. (1)). Hydrolysis of the reaction mixture leads to di(pyridyl)phosphane [15].

$$Py_3P + Li \xrightarrow[-0.5\ BiPy]{THF} \underset{\mathbf{1}}{[(THF)_2Li(Py)_2P]} \xrightarrow[-LiOH]{H_2O} Py_2PH \qquad (1)$$

The cleavage of a P–aryl bond seems to be the initial step leading to $LiPy_2P$ and 2-pyridyllithium. The latter product undergoes ligand coupling reaction and metal transfer to excess Py_3P to give $LiPy_2P$ and 2,2′-bipyridyine. The dimethyl aluminium derivative [Me_2AlPy_2P] (**2**) can be obtained either by treating Py_2PH with trimethyl aluminium or by the transmetalation reaction of [$(THF)_2LiPy_2P$] (**1**) with dimethyl aluminium chloride in diethyl ether/*n*-hexane (Eq. (2)). [Me_2AlPy_2P] (**2**) crystallises at 3 °C.

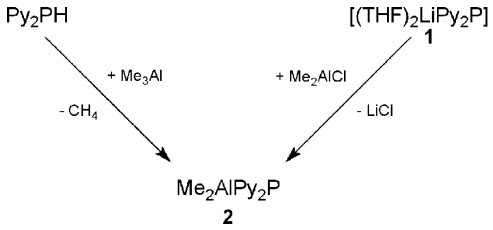

(2)

Fig. 1, left, illustrates the tetrahedral environment of the central lithium atom, which is coordinated by both pyridyl nitrogen- and two THF oxygen atoms. The Li–N distances are equally long and correspond to Li–N distances in lithium salts of 2-pyridyl substituted carbanions. The anion is almost planar and the geometrical features indicate delocalisation of the negative charge throughout the phosphanide. Like the anions depicted in Chart 3, [$(THF)_2LiPy_2P$] (**1**) exhibits no Li–P contacts. In the monomeric complex [Me_2AlPy_2P] (**2**) the aluminium and phosphorus atoms are μ_2-bridged by two pyridyl ring systems (Fig. 1, right). The $(THF)_2Li$-unit in **1** is replaced by a Me_2Al-fragment. The phosphorus atom is two-coordinated and the two P–C bond lengths are very similar, indicating delocalisation of the negative charge throughout the anion. The aluminium atom shows a distorted tetrahedral coordination sphere. Both Al–N bonds are of the same length.

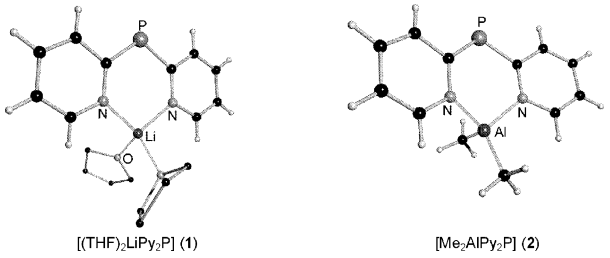

Fig. 1. The solid-state structures of [$(THF)_2LiPy_2P$] (**1**) and [Me_2AlPy_2P] (**2**).

However, the comparison of both complexes already reveals the coordination flexibility of the Py_2P^- anion in response to the different metal radii. While the lithium atom in **1** is in the plane of the anion, the aluminium atom in **2** is displaced from that plane and the complex adopts a butterfly arrangement [16]. Fig. 2 illustrates the gradual displacement of the Py_2E^- anion (E = CH, N, P, As) from planarity while coordinated *via*

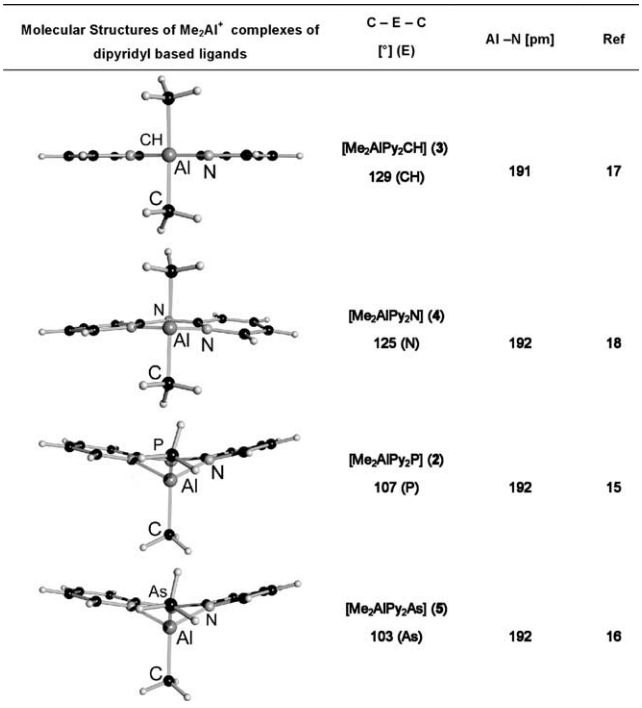

Fig. 2. The solid-state structures of the di(pyridyl)methanide (**3**) [17], -amide (**4**) [18], -phosphanide (**2**) [15] and -arsenide (**5**) [16] all containing the Me_2Al^+ cationic fragment. Although the Al–N distance is almost invariant in all structures the more acute C–E–C angle (As < P < N < CH) forces the complex in a more pronounced butterfly arrangement.

both ring nitrogen atoms to the structural standard Me_2Al^+ proceeding from [Me_2AlPy_2CH] (**3**) [17], [Me_2AlPy_2N] (**4**) [18], [Me_2AlPy_2P] (**2**) [15] to [Me_2AlPy_2As] (**5**) [16]. A view along the E···Al axis of the di(pyridyl) systems illustrating the deviation from planarity on coordination. In any case, a monomeric compound similar to the corresponding phosphorus analogue **2** is formed. Only the pyridyl nitrogen atoms coordinate the metal centre leaving the bridging atom separated from the cation. Geometric differences occur with respect to the ligand planarity when comparing the respective Group 13 complexes. While the C(H) analogous ligand system remains planar without exception the corresponding Group 15 derivatives of aluminium reveal a distinct deviation of the anion from planarity. In [Me_2AlPy_2P] (**2**) and the isomorphous [Me_2AlPy_2As] (**5**) complex the pyridyl ring planes intersect at an angle of 155°. The bridging angle C–E–C becomes more acute: 110.4(2)° (E = P, M = Li), 106.6(1)° (E = P, M = Al) and, as a consequence of the increased p-character in the C–As bonds, 103.0(3)° (E = As, M = Al). In addition, the intramolecular N···N′ distance (the 'bite') of the ligand differs in both phosphorus compounds (306.4 pm when E = P, M = Li (**1**) and 292.2 pm when E = P, M = Al(**2**)). The Al–N distance in all complexes **2**–**5** is almost invariant (192 pm) [5].

While the required coordination flexibility of the Py_2P^- anion guarantees accommodation of various different sized metal cations, the Lewis basicity of the central phosphorus atom is still to be discussed. In accordance to the electropositive nature of the bridgehead atoms all di(pyridyl) substituted anions behave like amides with the electron density accumulated at the ring nitrogen atoms rather than carbanions, phosphanides or arsenides. The divalent bridging atoms (N, P, As) in the related complexes should in principle be able to coordinate either one or even two further Lewis acidic metals to form heterobimetallic derivatives. According to the mesomeric structures (Scheme 1) it can act as a $2e^-$ (**a,c**) or even a $4e^-$ donor (**b**) [19].

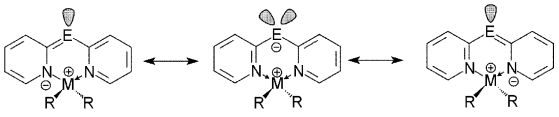

Scheme 1. Resonance forms of the Py_2E^- anions (E = N, P, As; $MR_2 = AlMe_2$).

Theoretical calculations, supported by experiments, have shown that while in the amides (E = N) the amido nitrogen does act as a typical Lewis base [20], the situation in the corresponding phosphanides (E = P) is different (Fig. 3). In the latter nearly all the charge density couples into the pyridyl rings leaving the central phosphorus atom only attractive for soft metals in the form of a π-acid type of coordinating centre. The Lewis basicity of the central bridging nitrogen atom in the di(pyridyl) amide is still high enough to coordinate a second equivalent of $AlEt_3$. The reaction of $[Et_2AlPy_2N]$ with $AlEt_3$ gives $[Et_2AlPy_2N \rightarrow AlEt_3]$ (**6**), while $[Et_2AlPy_2P]$ (**7**) forms no adduct under the same conditions. This further suggests that due to the higher electronegativity of the central nitrogen atom compared to the bridging divalent phosphorus atom the di(pyridyl)amide is the harder Lewis base.

In order to test the coordination abilities further, we reacted the pyridyl phosphanides with two contrasting type of metals viz Cs(I) and Fe(II) [21]. Towards the soft caesium metal in the complex $[(PMDETA)CsPy_2P]_2$ (**8**) ($PMDETA = (Me_2NCH_2CH_2)_2NMe$) an unprecedented coordination behaviour of the di(pyridyl)phosphanide ligand is observed. In this complex the ligand is involved *simultaneously* in a σ (through P and N) as well as a π (through the P–C–N segment) interaction with the caesium ions. This phospha-aza-allylic coordination represents an entirely new facet of coordination capability of the pyridyl phosphanide ligands. The reaction of di(pyridyl)phosphane Py_2PH with caesium metal in the presence of PMDETA afforded the dimeric complex **8** (Eq. (3)).

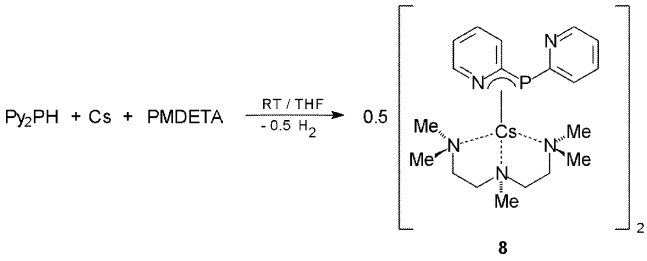

(3)

The phosphorus and one ring nitrogen atom is involved in a σ-type of interaction with caesium. At the same time a second caesium ion of the dimeric complex is η^3-coordinated to the phospha-aza-allylic P–C–N moiety in a π-type of interaction (Fig. 4). One pyridyl nitrogen atom on each of the Py_2P^- ligand remains non-coordinated. The P–C bond lengths in the anion are not affected by the metal coordination and identical within estimated S.D.'s and as long as in other metal di(pyridyl)phosphanides. Even the P–Cs distances are only marginally different and are similar to other caesium phosphanides. It is only in the N–Cs distances where the different bonding mode is mirrored in different lengths (σ-coordination is 16 pm shorter than the π-coordination). The Cs–C bond is as short as found in Cs-η^6 carbon coordination and considerably shorter than to terphenyl substituted phosphanides. Hence the P,C,N–Cs π bonding has to be considered a phospha-aza-allylic coordination with the negative charge not only delocalized to the coordinated ring but also to the phosphorus atom. This clearly proves the anticipated ability of the phosphorus centre in the Py_2P^- anion to coordinate soft metals. This is further substantiated in the structure of $[\{Cp(CO)_2Fe\}_2PPy_2][BMe_4]$ (**9**). In **9** the phosphorus atom of the ligand bridges two Fe(II) centres without any further Fe–N contacts. In an attempt to prepare heterobimetallic compounds we have reacted the aluminium derivative $[Me_2Al(Py_2P)]$ (**2**) with $[CpFe(CO)_3][BF_4]$ where in general a carbonyl group can easily be replaced by a phosphane. We aimed to utilise the vacant phosphorus site for coordination with Fe(II) while retaining the Al–N bonds. However, the Al–N bonds in the complex are cleaved presumably by the formation of the thermodynamically favourable AlF_3 accompanied by the alkylation of the tetrafluoroborate anion. This leads to the formation of $[\{Cp(CO)_2Fe\}_2PPy_2][BMe_4]$ (**9**) [21]. Two soft Lewis acidic metal fragments $[CpFe(CO)_2]^+$ are bridged by the phosphorus atom of a single di(pyridyl)phosphanide ligand to give the $[\{Cp(CO)_2Fe\}_2\{(\mu\text{-}P)Py_2\}]^+$ cation.

In conclusion the di(pyridyl)phosphanide ligand shows a metal-dependent coordination response and is involved in a highly unusual σ/π interaction with the caesium ion. The latter is clearly reminiscent of the

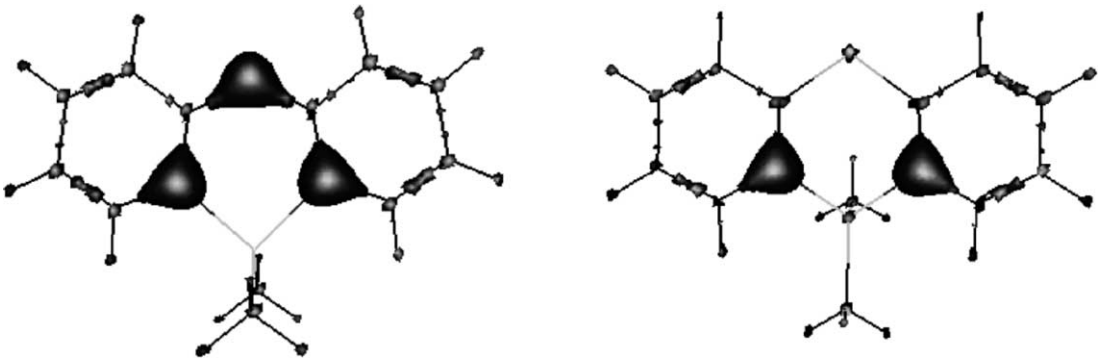

Fig. 3. The calculated total electron density at the 2.0 e $Å^{-3}$ level shows considerable Lewis base abilities at the central nitrogen atom in $[Me_2AlPy_2N]$ (**4**) (left) while at the central phosphorus atom of $[Me_2AlPy_2P]$ (**2**) hardly any electron density is left (right).

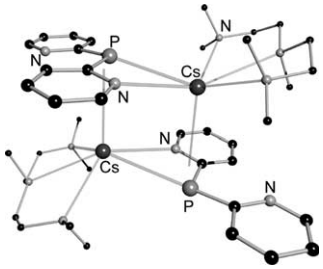

Fig. 4. The solid-state structure of $[(PMDETA)CsPy_2P]_2$ (**8**).

coordination of an allylic type of ligand. On the other hand, the phosphorus atom in the Py_2P^- anion is Lewis basic enough to bridge two soft iron metal centres. Again, the structure determining influence of different metals is obvious. Although calculations of a single molecule in the gas phase at 0 K suggest there is not much electron density left at the bridging phosphorus atom in $[Me_2Al(Py_2P)]$ (**2**) it rests on the organometallic fragment in the reaction mixture to shift charge density to either face of the *Janus Head* ligand (i.e. to the P- or the N-coordination site) [5].

2.1. Reactivity of tri(pyridyl)iminophosphorane versus tri(phenyl)iminophosphorane [23,24]

The different metal coordination in the *Janus Head* ligand periphery caused by the pyridyl substituents should obviously alter and augment the reactivity of the pyridyl substituted species in comparison to the e.g. phenyl substituted compounds. The compounds we picked for comparison were the tri(phenyl)iminophosphorane $Ph_3P{=}NSiMe_3$ (**10**) and the tri(pyridyl)iminophosphorane $Py_3P{=}NSiMe_3$ (**11**). The first is known since the landmark work of Staudinger by reacting triphenylphosphane with one equivalent of trimethylsilylazide (Eq. (4)) [22]. $Py_3P{=}NSiMe_3$ (**11**) can be obtained in an analogous reaction in high yield (Eq. (5)) [23].

$$Ph_3P + N_3SiMe_3 \xrightarrow[-N_2]{160\ ^\circ C\ /\ 6\ h} Ph_3P{=}NSiMe_3 \quad (4)$$

10

$$Py_3P + N_3SiMe_3 \xrightarrow[-N_2]{160\ ^\circ C\ /\ 6\ h} Py_3P{=}NSiMe_3 \quad (5)$$

11

Both, $Ph_3P{=}NSiMe_3$ (**10**) and $Py_3P{=}NSiMe_3$ (**11**), can be regarded as formally unsaturated P(V)–N compounds and hence as N analogues to phosphorus ylides or phosphane oxides. The isoelectronic derivatives **10** and **11** were reacted with methyllithium and the structures of the resulting lithium compounds were determined (Eqs. (6) and (7)) [24].

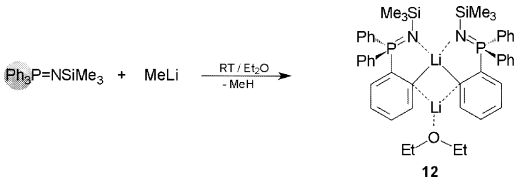

(6)

12

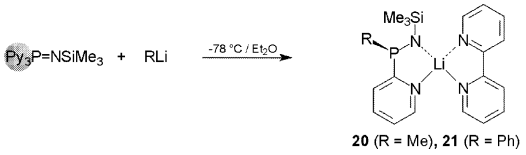

(7)

20 (R = Me), **21** (R = Ph)

The result from Eq. (6) is revealed by X-ray structure analysis shown in Fig. 5. The molecule of $[Li\{o\text{-}C_6H_4P(Ph_2)NSiMe_3\}]_2\cdot Et_2O$ (**12**) consists of two $Ph_3P{=}NSiMe_3$ iminophosphorane moieties each deprotonated in the *ortho* position of one phenyl ring. These single units dimerize by chelating with the *ortho* carbon

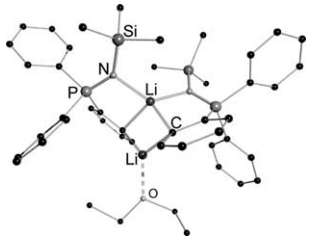

Fig. 5. The solid-state structure of $[Li\{o\text{-}C_6H_4P(Ph_2)NSiMe_3\}]_2\cdot Et_2O$ (**12**).

atoms and the imino-N donor centres a single central lithium atom. The second lithium ion is coordinated to both *ortho* ring carbon atoms and the oxygen atom of a diethyl ether molecule. The dimeric molecule adopts almost local C_2-symmetry. It matches all the requirements of an organometallic ligand capable of side-arm donation (Chart 4a): the deprotonated *ortho* phenyl carbon atom leads to metal–carbon σ bonds in reactions with metal halides and the $Ph_2P{=}NSiMe_3$ moiety donates an electron pair to that metal *via* the imine

Chart 4. Classical C-amino side-arm donation (a) comparable to P-imino side-arm donation (b).

nitrogen atom (Chart 4b).

3. σ-C–M bonds with imino side-arm donation [25–27]

The side-arm donation concept has been applied to stabilise Sn(II) centres by formation of Sn←N donor bonds in stannylenes and plumbylenes. The heavy carbene analogues have attracted continued interest. As examples of the plumbylenes are still rare we embarked on the synthesise of the tin and lead derivatives employing $[Li\{o\text{-}C_6H_4P(Ph_2)NSiMe_3\}]_2\cdot Et_2O$ (**12**) in salt elimination reactions. With $SnCl_2$ the diorgano tin complex $[Sn\{o\text{-}C_6H_4P(Ph_2)NSiMe_3\}_2]$ (**13**) was obtained, while the reaction with $PbCl_2$ gave the diarylplumbylene $[Pb\{o\text{-}C_6H_4P(Ph_2)NSiMe_3\}_2]$ (**14**) (Eq. (8)) [25].

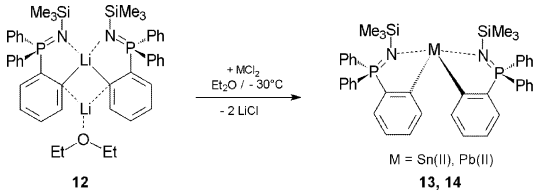

(8)

The structure of $[Sn\{o\text{-}C_6H_4P(Ph_2)NSiMe_3\}_2]$ (**13**) displays two Sn–C σ bonds and two Sn←N donor bonds in the monomer (Fig. 6). The two Sn–C distances fall in the range covered by other Sn–C(aryl) bonds in diarylstannylenes. The two Sn←N bond lengths differ by 8 pm. The C–Sn–C angle of 86.88(9)° is remarkably acute and to our knowledge it is the smallest ever observed in a diorganostannylene. This small value even below 90° is in accordance with the electronic configuration of a $^1\sigma^2$ singlet carbene homologue at Sn with the lone pair in a spherical s orbital and both bonding electrons in orthogonal p orbitals each. Normally the ideal 90° angle is expected to be widened by steric

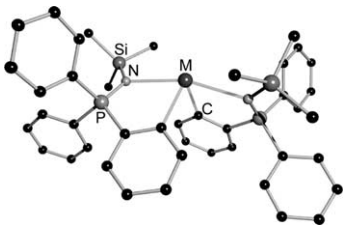

Fig. 6. The solid-state structures of the isostructural carbene homologues $[Sn\{o\text{-}C_6H_4P(Ph_2)NSiMe_3\}_2]$ (**13**) and $[Pb\{o\text{-}C_6H_4P(Ph_2)NSiMe_3\}_2]$ (**14**).

repulsion between the substituents. In **13**, however, it is squeezed below 90° due to parallel orientation of the bonded phenyl rings and $NSiMe_3$/phenyl repulsion of both substituents across the metal. Because of the limited bite of the ligand the N→Sn←N angle of 164.05(7)° is bent from linearity toward the bisection of the C–Sn–C angle. $[Pb\{o\text{-}C_6H_4P(Ph_2)NSiMe_3\}_2]$ (**14**) is isostructural to **13**. The two Pb–C distances match those found in other diarylplumbylenes. The Pb←N bond lengths are identical within estimated standard deviations. As anticipated, proceeding towards the higher homologue, the C–Pb–C angle of 86.0(2)° in **14** is even more acute than that in **13**. Because of the bigger radius and longer M–C bonds of lead compared to tin and the same bite of the ligand the N→Pb←N angle in **14** is only 162.8(2)° (Fig. 6).

In order to explore the general scope of the $(o\text{-}C_6H_4P(Ph_2)NSiMe_3)^-$ ligand system with a view to understanding its coordination behaviour towards diverse types of metals and metalloids we have carried out the reactions of $[Li\{o\text{-}C_6H_4P(Ph_2)NSiMe_3\}]_2\cdot Et_2O$ (**12**) with indium, germanium and iron halides [26]. In the choice of these reactions we had the following questions in mind:

i) How is the formal P=N double bond affected by *ortho* phenyl ring metallation and metal coordination?
ii) Can a metal ion accommodate more than two of these bulky ligands?
iii) Under which conditions would the imino nitrogen not participate in side-arm donation?
iv) What would be the mode of linkage to typical transition metal ions such as Fe(II) and Zn(II)?

The reactions of the lithiated iminophosphorane **12** with indium trichloride, ferrousdichloride or triphenylgermaniumchloride proceed quite smoothly by the complete replacement of chlorine atoms, with the elimination of lithium chloride and with the formation of three, two or one $M–C_{aryl}$ σ bonds to afford the products $[In\{o\text{-}C_6H_4P(Ph_2)NSiMe_3\}_3]$ (**15**), $[Fe\{o\text{-}C_6H_4P(Ph_2)NSiMe_3\}_2]$ (**16**) and $[Ph_3Ge\{o\text{-}C_6H_4P(Ph_2)\text{-}NSiMe_3\}]$ (**17**), respectively [26].

[In{*o*-$C_6H_4P(Ph_2)NSiMe_3$}$_3$] (**15**) is monomeric and the central indium atom is five-coordinate in a distorted trigonal-bipyramidal geometry. The coordination environment around indium is composed of three equatorial aryl substituents and two apical imino nitrogen atoms which function as side-arm donors. The third imino nitrogen is not involved in coordination to the indium atom. The sum of the equatorial bond angles is about 360°. Similar to the distortion in the equatorial bond angles the axial bond angle N1–In–N3 also deviates from the ideal value of 180° to 168.82(6)°. The In–C bond distances in **15** are similar to the In–C_{aryl} distances observed in other organoindium compounds despite the steric crowding. The In–N bond distances are considerably longer than those observed in more covalent situations. However, these can still be regarded as reasonably strong interactions considering the sum of the covalence radii of In (150 pm) and N (70 pm). In comparison the distance between In and the third pendent imino nitrogen atom of 354.2(2) pm clearly indicates the absence of any interaction between the two

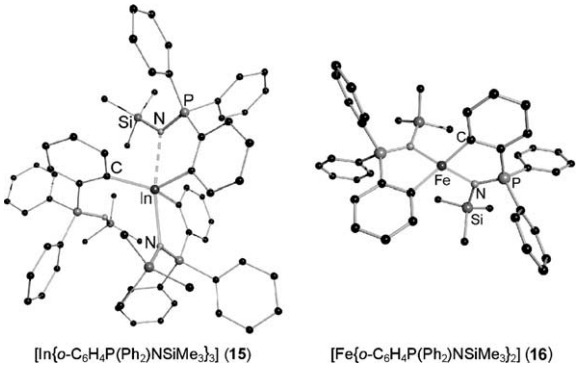

Fig. 7. The solid-state structures of [In{*o*-$C_6H_4P(Ph_2)NSiMe_3$}$_3$] (**15**) (left) and [Fe{*o*-$C_6H_4P(Ph_2)NSiMe_3$}$_2$] (**16**) (right).

atoms. The P–N bond distances are elongated by 2–3 pm upon metal coordination and the shorter distance involves the imino nitrogen that does not participate in coordination (Fig. 7, left).

The same is valid for the germanium complex [Ph_3Ge{*o*-$C_6H_4P(Ph_2)NSiMe_3$}] (**17**). The germanium atom is surrounded by four covalently bound carbon atoms. The side-arm nitrogen atom is at a distance of 311.1(4) pm from the central germanium atom. Although the bond angle N1–Ge1–C34 is 173.8°, close enough to be an axial angle, we discount the possibility of the side-arm nitrogen interacting with germanium on the following grounds: (1) Ge is out of plane by considerable 47 pm from an equatorial plane defined by Ge and the three *ipso* carbon atoms. (2) The sum of the equatorial bond angles is only 343.2° in comparison to the ideal value of 360.0°. (3) The bond distances found in molecules where the side-arm nitrogen is believed to participate in coordination to germanium are considerably shorter than those observed in the present instance (245–250 pm). The P–N bond distance in **17** is very similar to that in $Ph_3P{=}NSiMe_3$ (**10**) [22d] supporting the view of a non-coordinating imino nitrogen atom in **17**.

Although a large number of organoiron compounds containing 18 valence electrons are known the corresponding compounds with 14 valence electrons are not very abundant. The number of homoleptic iron(II) compounds containing alkyl or aryl ligands is also quite small in the literature. [Fe{*o*-$C_6H_4P(Ph_2)NSiMe_3$}$_2$] (**16**) belongs to this class of 14 VE type of molecules. The molecular structure of **16** is shown in Fig. 7, right [26]. The structure of the complex is isostructural with the other complex prepared with the *o*-$C_6H_4PPh_2NSiMe_3$ ligand viz [Zn{*o*-$C_6H_4P(Ph_2)NSiMe_3$}$_2$] (**19**) (vide infra). The coordination environment around Fe(II) is comprised of two carbon atoms and two nitrogen atoms arranged in a distorted tetrahedral geometry. The Fe–C distance observed is one of the shorter Fe–C distances that are found for organoiron(II) compounds. The Fe–N bond distances observed for **16** match those observed in compounds containing side-arm donation. Again, the P–N bond distance is slightly elongated because of metal coordination. Spectroscopic infrared and Raman investigations indicate for the ν(P=N) vibration a shift to higher wavenumbers upon N→M dative bonding [26].

The questions raised in the introduction can be answered as follows:

i) Density functional theory calculations and X-ray structure determinations (M = Li, Fe, In) find longer P–N bonds in the intramolecular metal complexed compounds than in the starting material. If the imino side-arm is not employed in metal coordination (M = Ge) the P=N bond is as short as in the starting material.

ii) The big trivalent indium atom clearly can accommodate three bulky ligands. The imino side-arm is flexible enough to fill vacant coordination sites or to act as a pendant spectator.

iii) Like in most coordination compounds, the presence of a dative bond is predominantly governed by steric conditions (i.e. the radius of the metal). In the indium complex there is not enough room for the third imino group to coordinate the metal, but in the germanium complex there would be plenty of space. Although the orientation of the three phenyl groups indicate the release of a vacant coordination site the imino group would not coordinate as the Lewis acidity of the central germanium atom is not high enough because of the lack of electron withdrawing substituents (e.g. Cl).

iv) The imino side-arm donation can be employed to stabilise a rare example of a 14-VE iron complex.

Among the d-block metals Cu(I) species play a leading role in regio- and stereoselective synthesis. The growing number of cuprates and organocopper compounds characterised by X-ray structure analysis is obvious. Organo copper(I) compounds CuR are generally encouraged as polynuclear species, which exist either as discrete aggregates or as polymers. Transformation of these aggregates and polymers to units of lower nuclearity can either be achieved by employment of very bulky groups R or by application of suitable Lewis bases. N, P, O, or S donor centres as well as alkynes have been reported to stabilise copper(I) species in low aggregation degrees. Hence, the $(o\text{-}C_6H_4P(Ph_2)NSiMe_3)^-$ anion seems to be a good candidate to stabilise a organo Cu(I) complex due to the integrated side-arm donation ability. In a salt elimination reaction of $[Li\{o\text{-}C_6H_4P(Ph_2)NSiMe_3\}]_2\cdot Et_2O$ (**12**) with CuBr the dimeric organo copper complex $[Cu\{o\text{-}C_6H_4P(Ph_2)NSiMe_3\}]_2$ (**18**) is obtained (Eq. (9)) [27].

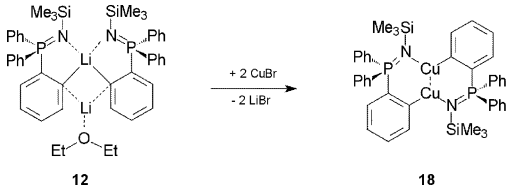

12 18 (9)

In **18** both lithium atoms from the C_2 symmetric starting material **12** are replaced by copper atoms to give a C_i symmetric dimer. Each copper atom is coordinated to an *ortho* carbon atom and the nitrogen atom of the $Ph_2P{=}NSiMe_3$ side-arm of a second ligand. It acts as an intermolecular rather than an intramolecular donor function. The Cu–C distance in **18** fall at the short end of the range observed in organo copper compounds. The Cu–N distances match almost perfectly the values of Cu–N distances in secondary copper amides $[CuNR_2]_4$. Therefore, the Cu-imine donor bond in **18** is as short as a Cu-amide bond. The former are probably widened by the higher coordination number at the copper centres (coordination number 4–6) compared to the coordination number two at copper in **18**. The P=N bond is about 5 pm longer than in the parent iminophosphorane $Ph_3P{=}NSiMe_3$ (**10**) [22d]. The Cu···Cu distance of 248.79(14) pm in complex **18** is rather short, both as a consequence of the bite of the bridging A-frame ligand which forces the metal centres into close proximity and metal d^{10}–d^{10} closed shell attraction. Although this distance is not remarkably short, the non-linear C–Cu–N angle of 167.8(2)° clearly indicates metal–metal interaction. One would expect the metals to be pushed further out of the centre (i.e. further away from the centre of inversion located in the middle of the Cu···Cu vector) and a bent of the C–Cu–N unit in the opposite direction if there was no 'sticky' interaction. This could easily be achieved by rotation of the metallated phenyl rings about the P–C(*ipso*) bonds. Steric requirements do not constrain the tilt of both monomeric units and the found lean could be maximised if the two metal cations would favour separation (Fig. 8) [27].

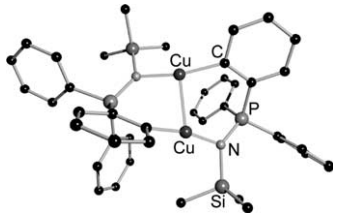

Fig. 8. The solid-state structure of $[Cu\{o\text{-}C_6H_4P(Ph_2)NSiMe_3\}]_2$ (**18**).

Organo zinc reagents in general are less reactive than Grignard reagents, a property that is a distinct advantage when more gentle reaction conditions are required. Diorgano zinc compounds containing functional substituents divide into two groups, i.e. compounds containing substituents which do not interact directly with the central zinc atom, and compounds in which coordination of the heteroatoms of the substituents is observed. The complex $[Zn\{o\text{-}C_6H_4P(Ph_2)NSiMe_3\}_2]$ (**19**) belongs to the second group, because both nitrogen atoms of the two $Ph_2P{=}NSiMe_3$ side-arms coordinate the zinc atom. The $o\text{-}C_6H_4PPh_2NSiMe_3^-$ ligand in **19** is closely related to other bidentate monoanionic (*C*,*N*)-chelating ligands. The structure of $[Zn\{o\text{-}C_6H_4P(Ph_2)NSiMe_3\}_2]$ (**19**) resembles widely the features already discussed with $[Fe\{o\text{-}C_6H_4P(Ph_2)NSiMe_3\}_2]$ (**16**) (Fig. 7, right). The zinc atom in **19** is tetrahedrally coordinated by both carbon and nitrogen atoms of the two ligands. The metal atom resides on a centre of inversion. The Zn–C distance is comparable to the Zn–C distances of other diaryl zinc species. The P=N bond in **19** is 1.7 pm shorter than in **18**.

In conclusion the transmetalation of the *ortho*-lithiated triphenyl trimethyliminophosphorane $[Li\{o\text{-}C_6H_4P(Ph_2)NSiMe_3\}]_2\cdot Et_2O$ (**12**) gives access to side-arm N-donating A-frame ligands in organometallic chemistry. The N donor bond can be as short as a metal amide bond like observed in the dimeric copper(I) complex $[Cu\{o\text{-}C_6H_4P(Ph_2)NSiMe_3\}]_2$ (**18**).

4. Reduction of tri(pyridyl)iminophosphoranes to phosphanamides [19,28]

Iminophosphoranes and polyphosphazenes are valuable building bocks in organo phosphorus chemistry and metal coordination. The P–N multiple bond and its transformation has always been the focus of reactivity studies and the crucial issue of commercially important materials. The presence of the pyridyl moiety in the place of *normal* alkyl or aryl substituents opens up additional avenues for interaction with transition or

main group metal ions apart from providing unexpected reactivity behaviour in the form of P–aryl bond cleavage reactions.

The contrasting reactivity behaviour of the two types of iminophosphoranes $Py_3P{=}NSiMe_3$ (**10**) (Eq. (7)) and $Ph_3P{=}NSiMe_3$ (**11**) (Eq. (6)) towards organo lithium reagents has prompted us to investigate these reactions and to establish access to chiral phosphanamines. The reaction of **11** with methyllithium gives [(2-2′-BiPy)LiPyP(Me)$NSiMe_3$] (**20**) and with phenyllithium affords the product [(2-2′-BiPy)LiPyP(Ph)$NSiMe_3$] (**21**). This products contain only *one* pyridyl substituent at the phosphorus atom. On the other hand, the reaction of $Py_3P{=}NSiMe_3$ (**11**) with 2-pyridyllithium affords $[Li(Py_2PNSiMe_3)]_2$ (**22**) where the phosphorus atom is bonded to *two* pyridyl substituents (Eq. 10).

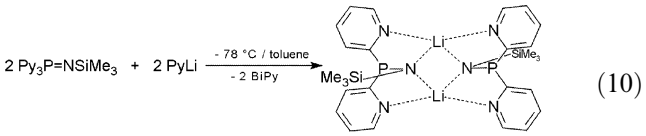

(10)

11 **22**

The X-ray structure of [(2-2′-BiPy)LiPyP(Ph)$NSiMe_3$] (**21**) is shown in Fig. 9, left. The structure of **20** is similar to that of **21** and can be described as a *spirocycle* around a lithium ion. The lithium ion is four coordinated and forms two five-membered metallacyles as a result of coordination by two chelating ligands, the bipyridine and the pyridylphosphanamide ligands. The P–N bond length in [(2-2′-BiPy)LiPyP(Ph)$NSiMe_3$] (**21**) of 163.5(3) pm is similar to that found for [(2-2′-BiPy)LiPyP(Me)N-$SiMe_3$] (**20**) and $[Li(Py_2PNSiMe_3)]_2$ (**22**). This value is considerably longer than that observed for $Py_3P{=}NSiMe_3$ (**11**) viz 152.8(2) pm [23], commonly interpreted as a greater double bond character, even if a bond shortening of 3–4 pm has to be attributed to the higher oxidation state of the phosphorus atom in **11** compared to **20**, **21** and **22**. It may be noted that the accepted value for a P–N single bond distance is about 170 pm whereas the P=N double bond distances found in various types of situations lie between 147 and 162 pm. [$Li(Py_2PN$-$SiMe_3)]_2$ (**22**) is a dimer of the lithium salt of di(pyridyl)phosphinotrimethylsilylamine. The structure is built around a Li_2N_2 core, the ubiquitous structural motif found in lithium amides. Apart from the Li_2N_2 four-membered ring, the structure consists of four five-membered metallacycles. Both lithium ions are tetracoordinate as a result of coordination of two chelating Py–P–N($SiMe_3$) moieties (Fig. 9, right) [28].

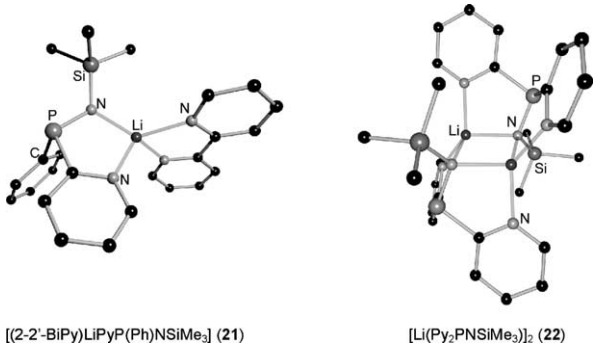

Fig. 9. The solid-state structures of [(2-2′-BiPy)LiPyP(Ph)$NSiMe_3$] (**21**) (left) and $[Li(Py_2PNSiMe_3)]_2$ (**22**) (right).

Replacement of the aryl groups in parent triorgano iminophosphoranes by pyridyl groups extends the coordination flexibility and as a result the reactivity of this class of compounds considerably. The nitrogen atom(s) in the substituents periphery co-operate in the metal coordination and facilitate P–Py bond cleavage. It was shown [28] that pyridyliminophosphoranes with phosphorus in the oxidation state (V) can easily be reduced to phosphanamides with phosphorus in the oxidation state (III) in a one pot reaction *via* double P–C bond cleavage. Addition of the carbanion from the organo lithium reagent and hydrolysis gives access to chiral phosphanamines, not trivial to make on different routes. Mechanistic studies from the $Py_nPh_{3-n}P{=}NSiMe_3$, $n = 1, 2, 3$, species suggest in accordance with computational anticipation that in the course of the reaction with RLi always PyLi is formed even at low temperature, subsequently eliminated from the complex. A 'hypervalent' five coordinated phosphorus atom is not required to rationalise the mechanism.

5. Reduction of tri(phenyl)iminophosphoranes to phosphanamines [29]

While the dual P–C bond cleavage with the pyridyl substituents at the central phosphorus atom in $Py_3P{=}NSiMe_3$ (**11**) represents a unique route to chiral phosphanamines, the P–C bond cleavage in $Ph_3P{=}NSiMe_3$ (**10**) requires harsher reaction conditions than the addition of organolithiums to the starting material. Refluxing **10** with elemental sodium in a THF suspension affords single P–C bond cleavage and gives biphenyl and the crimson sodium di(phenyl)phosphanamide [$(THF)_3Na(Ph_2PNSiMe_3)$] (**23**). Hydrolysis of **23** leads to the corresponding amine $Ph_2PN(H)SiMe_3$ (**24**) (Eq. (11)) [29].

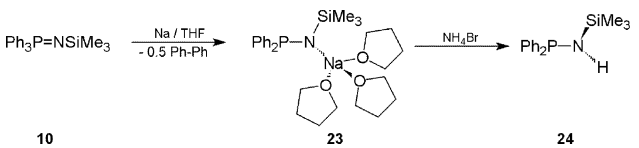

10 **23** **24**

(11)

In [$(THF)_3Na(Ph_2PNSiMe_3)$] (**23**) the $Ph_2PNSiMe_3^-$ anion coordinates as an amide in *s-trans*-conformation *via* the nitrogen atom to the sodium. The tetrahedral coordination sphere of the sodium atom is formed by

three additional THF molecules. The Na–N distance is that of a typical sodium amide while the P···Na distance of 335.9(4) pm is too long to be regarded a donor bond, the more the lone pair at the phosphorus atom points in the opposite direction, away from the metal (Fig. 10, left). The P–N bond of 163.6(8) pm in **23** is remarkably longer than the formal double bond in $Ph_3P{=}NSiMe_3$ (**10**) of 154.2(3) pm but still shortened by electrostatic reinforcement. The same is valid for the protonated form, the parent di(phenyl)phosphanamine $Ph_2PN(H)SiMe_3$ (**24**) (Fig. 10, right). The formal replacement of the sodium atom in **23** by a hydrogen atom only results

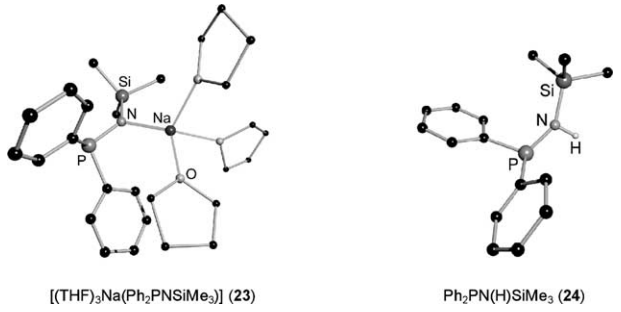

[(THF)$_3$Na(Ph$_2$PNSiMe$_3$)] (**23**) Ph$_2$PN(H)SiMe$_3$ (**24**)

Fig. 10. The solid-state structures of [(THF)$_3$Na(Ph$_2$PNSiMe$_3$)] (**23**) (left) and $Ph_2PN(H)SiMe_3$ (**24**) (right).

in a P–N bond elongation of 2.2 pm.

6. Reactivity of di(phenyl)phosphanamine

As a neutral molecule as well as the deprotonated *Janus Head* ligand with the phosphorus next to the nitrogen atom $Ph_2PN(H)SiMe_3$ (**24**) has two adjacent coordination sites. Dependent on the sterical demand and the Lewis acidity of the metal the ligand can serve as a N- and/or P-donor. The free ligand can be regarded a phosphanamide as well as an iminophosphanide. In response to the steric requirements the $Ph_2PNSiMe_3^-$ anion can either coordinate as the *s-cis*- or *s-trans*-conformer. $Ph_2PN(H)SiMe_3$ (**24**) reacts with one equivalent of $Zn\{N(SiMe_3)_2\}_2$ to give the dimer $[(Me_3Si)_2NZnP(Ph_2)NSiMe_3]_2$ (**25**). Different to **23** the ligand in **25** coordinates in the *s-cis* conformer *via* the phosphorus *and* the nitrogen atom to the zinc metal. A six-membered $Zn_2P_2N_2$ ring is formed. The additional $(Me_3Si)_2N^-$ anion at each zinc atom provides electroneutrality. This structure particularly emphasises the iminophosphidic mesomeric form of the anion (Scheme 2, Fig. 11, left). The reaction of **24** with elemental caesium leads to phosphorus–phosphorus bond formation in a reductive substituent coupling reaction to give polymeric $[(THF)Cs_2\{Ph(NSiMe_3)P\}_2]_n$ (**26**). Phosphorus(III) is reduced to a phosphorus(II) species. Metal coordination of the dianionic ligand $Me_3SiNP(Ph)P(Ph)NSiMe_3^{2-}$ is provided by the nitrogen atoms and

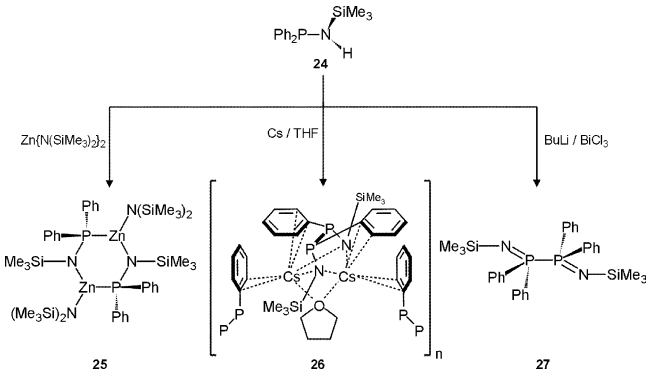

Scheme 2. Reactivity of the di(phenyl)phosphanamine $Ph_2PN(H)SiMe_3$ (**24**).

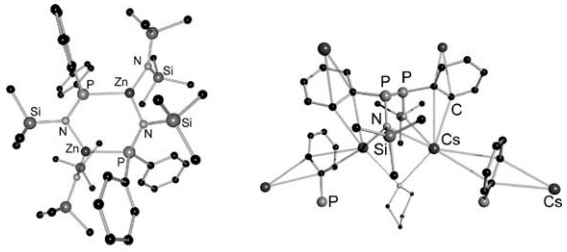

[(Me$_3$Si)$_2$NZnP(Ph$_2$)NSiMe$_3$]$_2$ (**25**) [(THF)Cs$_2${Ph(NSiMe$_3$)P}$_2$]$_n$ (**26**)

Fig. 11. The solid-state structures of $[(Me_3Si)_2NZnP(Ph_2)NSiMe_3]_2$ (**25**) (left) and $[(THF)Cs_2\{Ph(NSiMe_3)P\}_2]_n$ (**26**) (right).

not by the lone pair at the phosphorus atoms. Additional interaction of the soft metal to the phenyl π-systems to adjacent ligands encourages formation of a coordination polymer in the solid state (Scheme 2, Fig. 11, right). Oxidative substituent coupling to a P(IV) species occurs when $Ph_2PN(H)SiMe_3$ (**24**) is deprotonated with butyllithium first and subsequently reacted with bismuth trichloride. $(Ph_2PNSiMe_3)_2$ (**27**) and elemental bismuth is obtained (Scheme 2). Compound **27** shows two formal double bonds (P=N 154.1(2) pm) different to longer formal single P–N bonds in **25** (163.5(3) pm) and **26** (165.0(4) pm).

Similar to the reaction of $Ph_2PN(H)SiMe_3$ (**24**) with one equivalent of $Zn\{N(SiMe_3)_2\}_2$ to give the dimer **25**, **24** was reacted with $Sn\{N(SiMe_3)_2\}_2$ in THF at −78 °C (Eq. (12)).

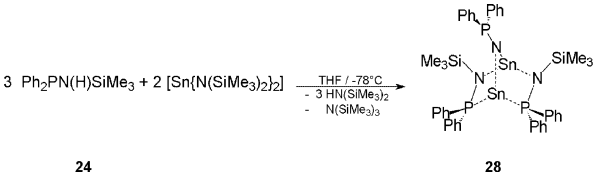

(12)

Although the recovered product $[Sn_2\{P(Ph_2)NSiMe_3\}\{NP(Ph_2)\}]_2$ (**28**) shows a central $Sn_2P_2N_2$ six-membered ring as well, the structure is considerably different to the zinc derivative **25**. In the ring the two $Ph_2PNSiMe_3^-$ anions in the *s-cis* conformation are

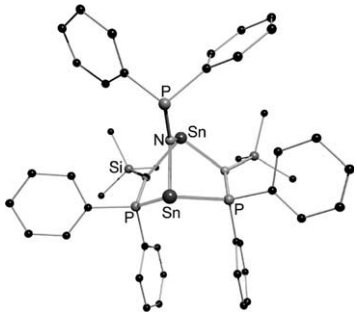

Fig. 12. The solid-state structure of $[Sn_2\{P(Ph_2)NSiMe_3\}\{NP(Ph_2)\}]_2$ (**28**).

organised in a head-to-head arrangement. One tin atom is coordinated to both phosphorus atoms while the other to both nitrogen atoms of the ligands. Rather than by two di(trimethylsilyl)amide anions in **25** in this compound electroneutrality is provided by a single imidophosphanide dianion $[Ph_2PN]^{2-}$. The nitrogen atom bridges both tin atoms across the ring resulting in a connectivity reminiscent to norbornadiene. As the ring nitrogen atoms coordinate just one tin metal the P–N bond length is on average 164.0 pm while that one involved in bridging is longer (167.8(6) pm), because the negative charge is to be shared between two electropositive centres (Fig. 12).

7. Aminoiminophosphoranes [30–32]

Monoanionic chelating ligand systems $[R–N–E–N–R]^-$ with E = $Si(R_2)$, $S(R_2)$ or S(R), C(R), and $P(R_2)$ are of significant interest as versatile chelating ligands. Of these the aminoiminophosphoranates $[Me_3Si–N–P(R_2)–N–Me_3Si]^-$ deserve special mention. These ligands are derived formally by the deprotonation of $Ph_2P\{N(H)SiMe_3\}(NSiMe_3)$ (**29**). The resulting chelating anion is comparable in terms of its cone angle to the ubiquitous $C_5Me_5^-$ ligand. By variation of the P-bonded organic groups specific properties of the corresponding metal complexes can be tuned sterically (i.e. *via* modification of the cone-angle of the ligand) and electronically. The presence of silylated substituents on nitrogen ensures solubility as well as steric protection to the coordinated metal ion. These desirable features have enabled the use of these ligands as building blocks for many transition and main group metal containing metallacycles. Further modification of the compounds is possible by invoking the reactivity of the $N–SiMe_3$ group. The starting material is obtained in the reaction of trimethylsilylazide with di(phenyl)phosphane in a Staudinger-type reaction [30]. The amino function of $Ph_2P\{N(H)SiMe_3\}(NSiMe_3)$ (**29**) can be deprotonated by strong bases (Scheme 3) [31]. The three chemically active sites in the *N*,*N*′-di(trimethylsilyl)-aminoimino-di(phenyl)phosphorane **29** are: (i) the acidic NH function; (ii) the donating imino nitrogen atom; and (iii) the potential cleavage of the Si–N or P–N bond, leading to anionic chelating ligands [32].

7.1. Di(phenyl)aminoiminophosphoranates [33,34]

The di(trimethylsilyl)di(phenyl)aminoiminophosphorane $Ph_2P\{N(H)SiMe_3\}(NSiMe_3)$ (**29**) reacts in THF with butyllithium to give $[(THF)_2Li\{(NSiMe_3)_2PPh_2\}]$ (**30**), with sodium hydride to give the highly reactive and low melting sodium sodiate $[Na(THF)_6][Na\{(NSiMe_3)_2PPh_2\}_2]$ (**31**), with potassium hydride to give $[(THF)_4K\{(NSiMe_3)_2PPh_2\}]$ (**32**), with elemental rubidium to give the dimer $[(THF)Rb\{(NSiMe_3)_2PPh_2\}]_2$ (**33**), and with caesium metal to give the polymer $[Cs\{(NSiMe_3)_2PPh_2\}]_\infty$ (**34**) in quantitative yields (Scheme 3) [33]. Surprisingly, the structural series of alkali metal aminoiminophosphoranates **30**–**34** is not so predictable as one might anticipate by considering the most homogeneous periodic properties of these metals. Most remarkably the sodium derivative **31** forms a sodium sodiate within a solvent separated ion pair. The maximum content of THF is reached with the potassium derivative **32** coordinating four molecules. Although the radius of both, the rubidium and caesium cations, are much bigger, their molecules prefer to aggregate rather than taking up more donating solvent. The caesium metal in **34** coordinates no THF as it favours to coordinate to the π-systems of the phenyl substituents, already noticed in $[(THF)Cs_2\{Ph(NSiMe_3)P\}_2]_n$ (**26**).

The structural appearance of the alkaline earth aminoiminophosphoranates $[(THF)_nM\{(NSiMe_3)_2PPh_2\}_2]$ (M = alkaline earth metal) (**35**–**39**) seems much more homogeneous. The amino function of $Ph_2P\{N(H)SiMe_3\}(NSiMe_3)$ (**29**) can readily be deprotonated by strong bases. In the syntheses presented here the alkaline earth metal di[bis(trimethylsilyl)amides] were used as bases. They can be obtained from the tin-di[bis(trimethylsilyl)amide]. The beryllium-di[bis(trimethylsilyl)amide] was obtained by a salt elimination reaction of the lithium derivative with beryllium dichloride. The barium-di[bis(trimethylsilyl)amide] was obtained by the reaction of bis(trimethylsilyl)amine with elemental barium [34]. The most obvious common structural feature of **35**–**39** is their monomeric molecular state, $[Be\{(NSiMe_3)_2PPh_2\}_2]$, (**35**), $[Mg\{(NSiMe_3)_2PPh_2\}_2]$, (**36**), $[(THF)Ca\{(NSiMe_3)_2PPh_2\}_2]$, (**37**) $[(THF)_2Sr\{(NSiMe_3)_2PPh_2\}_2]$, (**38**), and $[(THF)_2Ba\{(NSiMe_3)_2PPh_2\}_2]$, (**39**). This fact seems not surprising in view of the considerable steric demand of the two anions. They shield the dication quite well. There is only room for one or two THF molecules but not for oligomerisation (Scheme 4).

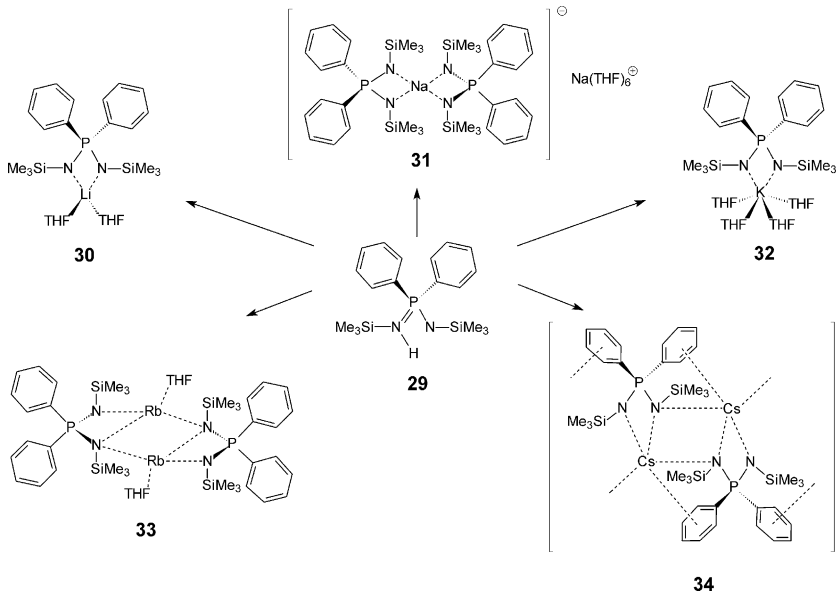

Scheme 3. Known structures of the alkali metal complexes **30**–**34** containing the $Ph_2P(Me_3SiN)_2^-$ ligand.

The question what factors govern the coordination geometry of the alkaline earth metal has to be answered in three parts:

i) Like in most compounds, as well the coordination geometry of the alkaline earth metals is governed by anion cation size (miss)match. Not surprisingly, the coordination number increases from four (Be, Mg) *via* five (Ca) to six (Sr, Ba). Two of the $Ph_2P(Me_3SiN)_2^-$ anions cover the coordination sphere of beryllium and magnesium, while with calcium one single THF molecule and with strontium and barium two additional THF molecules are required to complete the metal coordination sphere.
ii) Like in many other heavier alkaline earth metal complexes the anions in **35**–**39** were found to be *cisoid* with respect to each other. Even against steric strain the two THF molecules in **38** and **39** are coordinated to the same hemisphere of the metal. Apart from the ab initio MO computational prediction (significant covalent σ-bonding contributions involving metal d-orbitals and polarisation of the metal cation by the anions) there is now experimental evidence of a bent arrangement presented here (structural strain, shortening of the average P–N distance and NMR upfield shift).
iii) Although multihapto π interaction to an anion has been calculated to be favourable for the heavier alkaline earth metal cations, this effect has not yet been reported experimentally. Even against sterical strain the heavier alkaline earth metals Sr and Ba leave the plane of one anion in **38** and **39**,

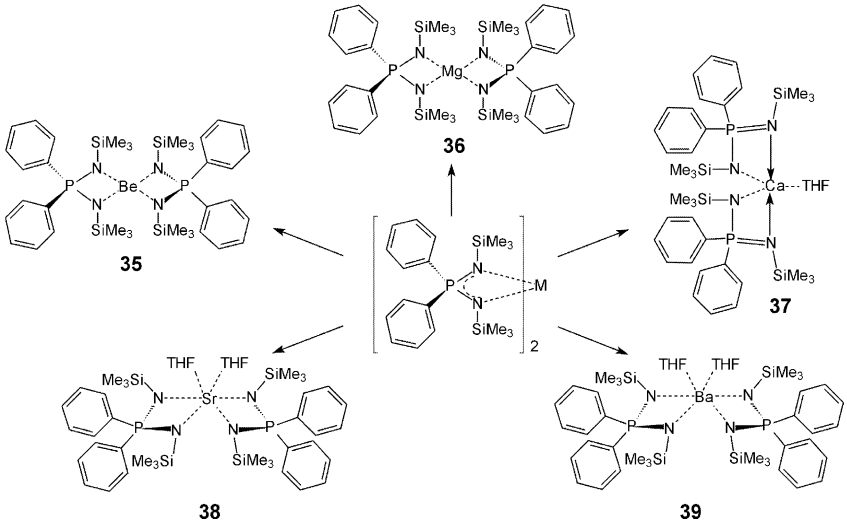

Scheme 4. Known structures of the alkaline earth metal complexes **35**–**39** containing the $Ph_2P(Me_3SiN)_2^-$ ligand.

demonstrating their preference to interact with π electron density. This effect can also be found in related systems. Certainly, the π interaction is smaller than in the alkaline earth metallocenes and counter-balanced by steric requirements but it is significant. The metal π interaction rises with the mass of the metal and decreasing bulk of the anion but is independent from *cisoid* or *transoid* arrangement of the anions [34].

8. Di(pyridyl)aminoiminophosphoranates [35]

The versatility of the above ligand systems can be enhanced by the construction of additional coordinating sites separated away from the anionic centre. Thus, the incorporation of the pyridyl substituents on the phosphorus centre in the place of the phenyl groups, alters and augments the coordination capability of the ligand system and leads to the design of multi-dentate *Janus Head* ligands. Different to the simple aminoiminophosphoranate anions the pyridyl derivatives would have two potential chelating sites, firstly the $[N–P–N]^-$ skeleton, predominantly accommodating the negative charge, and secondly the two remote nitrogen atoms in the pyridyl substituents. However, free rotation about the P–C_{ipso} bond can easily bring the pyridyl nitrogen atoms into a more proximal and convenient location for coordination. An additional possibility of a π interaction of the heteroaromatic ring to the metal also exists. In order to test these ideas we have designed and assembled the first example of a pyridyl substituted aminoiminophosphoranate type of ligand, $Py_2P\{N(H)SiMe_3\}(NSiMe_3)$ (**40**) (Eq. (13)) [35].

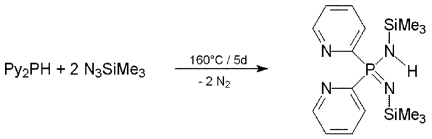

(13)

40

The molecular structure of the *N*,*N*′-bis(trimethylsilyl)aminoiminodi(pyridyl)phosphorane **40** is shown in Fig. 13 [35]. The two P–N bond lengths present in this molecule are not equal with P–N(H) being 164.9(2) and P=N being 152.9(2) pm. Thus both the bond lengths observed are smaller than the value for a standard P–N formal single bond. Also the bond angles around the two nitrogen atoms in $Py_2P\{N(H)SiMe_3\}(NSiMe_3)$ (**40**) point to their dissimilarity with each other. Thus, the Si–N(H)–P angle is 123.10(10)° whereas the corresponding angle at the imino nitrogen atom is 146.89(11)°, suggesting that the hybridisation at the latter has less p character than the former. The N(H) group in **40** interacts with a pyridyl nitrogen atom of an adjacent molecule leading to an interesting intermolecular hydrogen bonding in the form of N–H···N bridges. This results in the formation of a dimeric structure containing a 10-membered ring system. The metric parameters involved in the hydrogen bonding are quite reasonable with the N–H distance of 80.7(2) and H···N(Py) distance of 247.3(2) pm. The N–H···N motif is fairly linear as evidenced by a bond angle of 153.11(2)°. These parameters are in keeping with the hydrogen bonding trends known for N–H···N secondary interactions (Fig. 13).

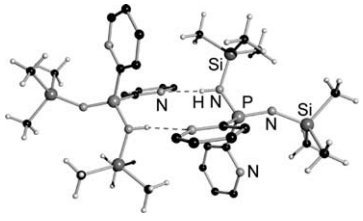

Fig. 13. The solid-state structure of $Py_2P\{N(H)SiMe_3\}(NSiMe_3)$ (**40**), depicting the arrangement of two molecules to enable the (Py)N···H–N($SiMe_3$) hydrogen bond.

Deprotonation of the N–H group by a strong base would generate a chelating NPN-unit. However, this coordination site would compete with the N(Py)–P–N(Py) chelating, already indicated by the (Py)N···H–N hydrogen bonding in the *Janus Head* ligand (Chart 2b). Useful metal precursors for this purpose are either metal amides or metal alkyls. Accordingly the reaction of **40** with $[M\{N(SiMe_3)_2\}_2]$ M = Sr or Ba proceeds quite smoothly at room temperature to afford the complexes $[(THF)Sr\{Py_2P(NSiMe_3)_2\}_2]$ (**41**) and $[(4\text{-}4'\text{-bipy})Ba\{Py_2P(NSiMe_3)_2\}_2]_n$ (**42**) (Eq. (14)). In an analogous manner dimethylzinc reacts with **40** and complete elimination of methane results in the formation of $[Zn\{Py_2P(NSiMe_3)_2\}_2]$ (**43**) (Eq. (15)).

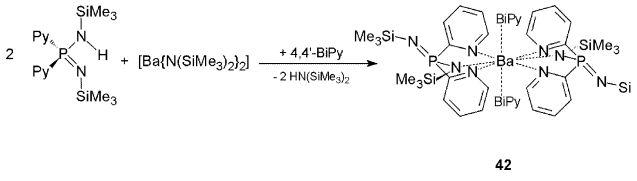

42

(14)

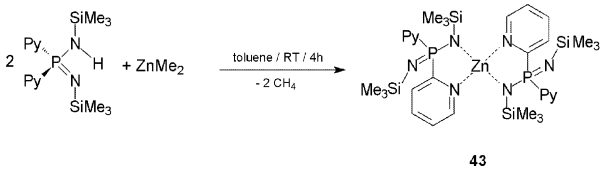

43

(15)

Single crystals of compound $[(THF)Sr\{Py_2P(NSiMe_3)_2\}_2]$ (**41**) have been obtained from a solution of THF/pentane at −18 °C. Complex **41** is a monomer in the solid state (Fig. 14) [35]. The structure in comparison to $[(THF)_2Sr\{(NSiMe_3)_2PPh_2\}_2]$ (**38**) explains excep-

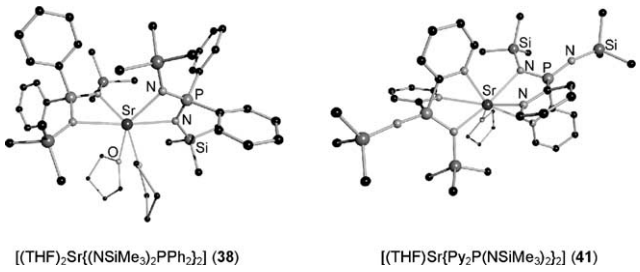

Fig. 14. The solid-state structure of $[(THF)_2Sr\{(NSiMe_3)_2PPh_2\}_2]$, (**38**) (left) in comparison to $[(THF)Sr\{Py_2P(NSiMe_3)_2\}_2]$ (**41**) (right).

tionally well the new facility of the pyridyl substituted ligand. While the di(phenyl)aminoiminophosphoranate is a (*N*,*N*) chelating ligand, the di(pyridyl)aminoiminophosphoranate is a tripodal ligand to the strontium dication. Two molecules of deprotonated **40** are coordinated to the strontium ion in a tripodal κ^3 mode. The amino hydrogen atom on each ligand reacts with the metal amide to form a M–N bond. The second imino nitrogen atoms of the ligand on the other hand do not interact with the metal ion. In contrast, however, *both* the pyridyl nitrogen atoms of each ligand are involved in coordination. Thus, the metal is enveloped by two ligands with a coordination environment of four pyridyl nitrogen atoms and two amido nitrogen atoms in a tripodal fashion. A seventh coordination site is occupied by a solvent THF molecule. The two tripodal chelating ligands coordinate to the strontium ion in nearly the same mode. Despite of this, within each ligand different Sr–N distances are found. The amido metal bonds are the shortest nitrogen–metal distances found in this molecule. The two pyridyl rings of each ligand differ in their coordination to the metal centre. Two pyridyl groups (one each from each ligand) that are *cisoid* form an acute angle when coordinated to strontium. The Sr–N(Py) distances are slightly longer than the strontium amide bond distances, as expected. The two remaining pyridyl rings also coordinate in a *cisoid* manner to the metal centre, but in contrast the angle they form on coordination to the metal ion is twice as wide. This coordinating situation enables the seventh coordinating moiety in the form of a solvent THF molecule to approach the metal ion comfortably to complete the hepta-coordination envelope around the strontium ion by fitting in perfectly between the two pyridyl groups. Although there is no space to accommodate a second THF molecule as at the hexa-coordinated strontium atom in $[(THF)_2Sr\{(NSiMe_3)_2PPh_2\}_2]$, (**38**) the coordination number increases in **41**.

The barium complex $[(4\text{-}4'\text{-BiPy})Ba\{Py_2P(NSiMe_3)_2\}_2]_n$ (**42**) derived from the di(pyridyl)aminoiminophosphorane $Py_2P\{N(H)SiMe_3\}(NSiMe_3)$ (**40**) was isolated in the presence of the added neutral Lewis base 4-4′bipyridine [35]. The compound could be crystallised from a mixture of toluene and tetrahydrofuran at −30 °C. Like in **42** the $Py_2P(NSiMe_3)_2^-$ anions act as tripodal ligands. Two of them are involved in coordination to the barium ion in a similar manner as observed for the strontium complex **41**. The 4-4′-bipyridine ligands, on the other hand, assist the formation of a polymeric zigzag structural arrangement of **42**. Thus, each barium dication in the polymeric chain is eight-coordinate. An interesting feature of the polymeric structure of $[(4\text{-}4'\text{-BiPy})Ba\{Py_2P(NSiMe_3)_2\}_2]_n$ (**42**) is that the two bipyridine ligands around each barium ion are not *exactly* opposite to each other. Such an arrangement would have led to a linear polymeric

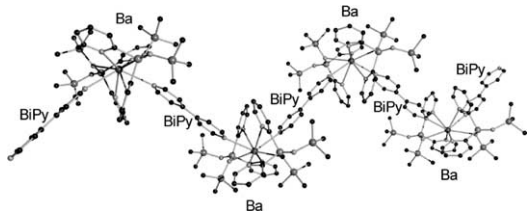

Fig. 15. The solid-state structure of $[(4\text{-}4'\text{-BiPy})Ba\{Py_2P(NSiMe_3)_2\}_2]_n$ (**42**), depicting the zigzag arrangement of $[Ba\{Py_2P(NSiMe_3)_2\}_2]$ moieties via linkage of 4-4′-bipyridine donors.

structure. Instead in the observed arrangement the (BiPy)N–Ba–N(BiPy) angle is substantially smaller (125.71(10)°) and leads to the organisation of the molecules into a zigzag type architecture (Fig. 15).

The molecular structure of the zinc complex $[Zn\{Py_2P(NSiMe_3)_2\}_2]$ (**43**) is shown in Fig. 16 [35]. Unlike compounds $[(THF)Sr\{Py_2P(NSiMe_3)_2\}_2]$ (**41**) and $[(4\text{-}4'\text{-BiPy})Ba\{Py_2P(NSiMe_3)_2\}_2]_n$ (**42**) where the metal ions contain ancillary ligands also, the coordination environment of zinc in $[Zn\{Py_2P(NSiMe_3)_2\}_2]$ (**43**) is entirely made up of two pyridyl aminoiminophosphoranate ligands. Also unlike in **41** and **42**, the $Py_2P(NSiMe_3)_2^-$ anions function as bidentate chelating ligands towards the zinc ion. One of the pyridyl nitrogen atoms and the imino nitrogen atom of the di(pyridyl)-aminoiminophosphoranate ligands are involved in coordination. Thus, the coordination around zinc is entirely composed of nitrogen atoms and the coordination geometry is approximately tetrahedral. The two Zn–N bond distances corresponding to the imino

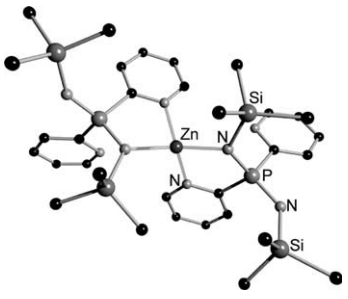

Fig. 16. The solid-state structure of $[Zn\{Py_2P(NSiMe_3)_2\}_2]$ (**43**).

nitrogen atoms are on average 10 pm shorter than the Zn–N(Py) distances. The first are similar to the one found in zinc cyclophosphazene while the second are comparable to other coordinating distances found for Zn–pyridine complexes.

In the complexes **41**, **42** and **43** the di(pyridyl)aminoiminophosphoranate $Py_2P(NSiMe_3)_2^-$ ligand utilises at least one pyridyl ligand in conjunction with an imino nitrogen for coordination. Even in the lithium complexes **20**–**22**, although the ligand is now truncated, a similar mode of coordination is seen. This reactivity behaviour distinguishes it from the di(phenyl)aminoiminophosphoranate ligand $Ph_2P(NSiMe_3)_2^-$ which in its reactivity acts as a $[NPN]^-$ ligand exclusively (Schemes 3 and 4). Presumably the reason for the different reactivity of **40** stems from the possibility of greater stability associated with a five-membered metallacycle that is formed by involving the pyridyl nitrogen atom in preference to the four-membered metallically formation that would occur if the imino nitrogen and the amido nitrogen atoms coordinate together. With barium and strontium ions which have a preference for larger coordination numbers deprotonated **40** acts as a tripodal ligand utilising both the pyridyl groups and the amido nitrogen atom. However, zinc which prefers a tetrahedral geometry with four ligands solicits and obtains a bidentate chelating mode from $Py_2P(NSiMe_3)_2^-$. These varied modes of coordination point to the flexible nature of the multi-dentate *Janus Head* ligand [35].

Among the various structural parameters of compounds **40**–**43** one point of interest is the variation and the difference in the two P–N bond lengths in the $Py_2P(NSiMe_3)_2$ moiety in the compounds. The largest difference is quite obviously in the native ligand containing the amino hydrogen atom (**40**). The P–N bond lengths here differ by 12.0 pm with the shorter bond length being 152.9(2) pm. This represents one extreme of the situation in which there is a more localised structure in terms of the P–N double and single bonds. As the amino group is deprotonated and the ligand is involved in the formation of the metallacycle the difference in the P–N bond lengths decreases. This is indicative of a growing delocalization of the negative charge over the entire fragment. A near complete delocalization is realised in the barium complex $[(4\text{-}4'\text{-BiPy})Ba\{Py_2P(NSiMe_3)_2\}_2]_n$ (**42**) where both the P–N bonds have nearly equal distance and the difference between them reduces to only 1.9 pm. The situation with the zinc complex $[Zn\{Py_2P(NSiMe_3)_2\}_2]$ (**43**) and the strontium complex $[(THF)Sr\{Py_2P(NSiMe_3)_2\}_2]$ (**41**) is intermediate in nature with the former closer to the ligand ($\Delta_{P-N} = 7.6$ pm) and the latter to that of the barium complex ($\Delta_{P-N} = 4.3$ and 5.1 pm). A similar trend is also noticeable in the two Si–N bond distances found for these compounds. Thus, in **40** the Δ_{Si-N} is 7.3 pm and it progressively decreases in **43** (6.2 and 2.4 pm), **41** (4.4 and 3.7 pm) and **42** (1.5 pm) consistent with the trend found in the P–N bond lengths. In contrast to these changes the P–C bonds remain completely unaffected from **40** to **43**. The bond angle variations, although smaller in magnitude in comparison to the bond length changes, also are consistent with the above arguments. It can be seen that the N–P–N angle widens upon metal coordination with the highest value being observed for the barium complex **42** (125.79(12)°). The C–P–C angles shrink upon coordination although the magnitude of change is only marginal. An interesting correlation is observed between the $P-N_{coord}-Si$ bond angle and the corresponding P–N bond. As the bond angle increases the P–N bond length decreases.

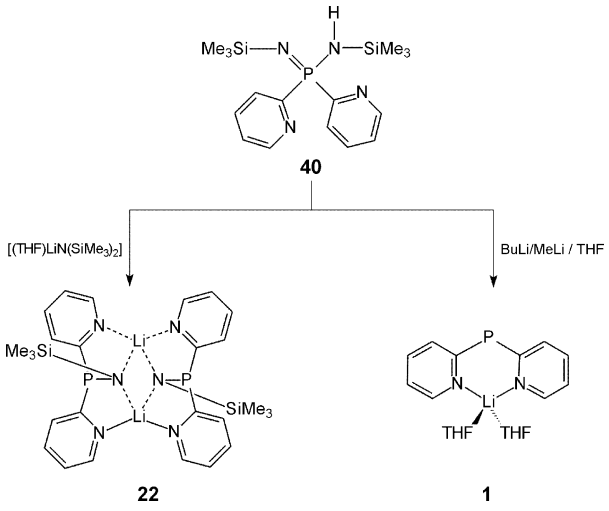

Scheme 5. The different reactivity of $Py_2P\{N(H)SiMe_3\}(NSiMe_3)$ (**40**) towards lithium disilylamide and lithiumorganics.

The reactions of organolithium reagents or lithium bis(trimethylsilyl) amide with $Py_2P\{N(H)SiMe_3\}(NSiMe_3)$ (**40**) proceed in an unexpected and entirely different manner in comparison to the reactions described above with alkaline earth or zinc reagents [35]. The mechanism of these reactions is quite complex and is not yet fully delineated. In the reaction of **40** with the lithium amide $[(THF)LiN(SiMe_3)_2]$ compound $[Li(Py_2PNSiMe_3)]_2$ (**22**) was isolated as the only product (Scheme 5). In this reaction a P–N bond is broken and the phosphorus centre is reduced to an oxidation state three.

In a sharp contrast to the reaction pathway found above, the reaction of **40** with *n*-butyl lithium or methyl lithium leads to the formation of the lithiumphosphanide $[(THF)_2LiPy_2P]$ (**1**). This reaction is quite remarkable. While one half of the ligand (N–P–N segment) undergoes bond scission involving the P–N bonds the other half of the ligand involving the Py–P–Py part remains unscathed. Phosphorus undergoes a reduction

accompanying the cleavage of both the P=N and P–N bonds. The lithium phosphanide (**1**) can be independently generated by the deprotonation of di(pyridyl)phosphane, Py_2PH with either *n*-butyl lithium or methyl lithium. Another route for the synthesis of compound **1** which we reported earlier is by a P–C bond cleavage of tri(pyridyl)phosphane using lithium metal (Eq. (1)). Although the cleavage of P–N bonds in the presence of organometallic reagents has been documented previously, particularly in the substitution reactions of halogenocyclophosphazenes, where the primary driving force for such reactions is the metal–halogen exchange reaction followed by the coordination of the metal ion by the nitrogen atoms of the ring, the type of reactivity seen in the present instance is completely unprecedented. Thus for example, analogous reactions with $Ph_2P\{N(H)SiMe_3\}(NSiMe_3)$ (**29**) proceed in a normal way with deprotonation without P–N bond scission and with the lithium ion being coordinated by the chelating NPN-unit.

9. Conclusion

Substitution of the organic alkyl or aryl groups in the classical $NP(R_2)N^-$ chelating anionic ligand by two pyridyl groups converts it into a *Janus Head* $NP(Py_2)N^-$ tripodal ligand. At least one pyridyl ring nitrogen in addition to only one imido nitrogen atom is used in metal coordination. The active ligand periphery opens up several avenues: (a) coordination site selectivity NPN^- versus (Py)N–PN(Py); (b) adaptability in ligation composition depending on the geometric constraints and coordination capability of the metals; and (c) the possibility of forming heterobimetallic complexes where the di(pyridyl) aminoiminophophoranes are employed as flexible metal linkers and not only as bulky protectants. Surprisingly, in pyridyl substituted aminoiminophophoranes it is easy to cleave either one or both P–N bonds. This reduction of P(V) species to P(III) compounds is very uncommon and supplies easy access to phosphanylamines and secondary phosphanes, not easy to make by different routes.

Acknowledgements

We thank the Deutsche Forschungsgemeinschaft and the Fonds der Chemischen Industrie for continuos financial support.

References

[1] (a) B. Cornils, W.A. Herrmann, Applied Homogeneous Catalysis with Organometallic Compounds, Wiley-VCH, Weinheim, 2002; (b) M. Beller, Transition Metals for Organic Synthesis, Wiley-VCH, Weinheim, 1998.
[2] H. Yamamoto, Lewis Acid Reagents—A Practical Approach, Oxford University Press, Oxford, 1999.
[3] (a) J. Storre, T. Belgardt, D. Stalke, H.W. Roesky, Angew. Chem. 106 (1994) 1365;
(b) J. Storre, T. Belgardt, D. Stalke, H.W. Roesky, Angew. Chem. Int. Ed. Engl. 33 (1994) 1244;
(c) J. Storre, A. Klemp, H.W. Roesky, H.-G. Schmidt, M. Noltemeyer, R. Fleischer, D. Stalke, J. Am. Chem. Soc. 118 (1996) 1380;
(d) J. Storre, A. Klemp, H.W. Roesky, R. Fleischer, D. Stalke, Organometallics 16 (1997) 3074;
(e) H.W. Roesky, H.-G. Schmidt, M. Noltemeyer, R. Fleischer, D. Stalke, J. Am. Chem. Soc. 119 (1997) 7505.
[4] (a) L.D. Quin, A Guide to Organophosphorus Chemistry, Wiley & Sons, New York, 2000;
(b) K.B. Dillon, F. Mathey, J.F. Nixon, Phosphorus: The Carbon Copy, Wiley-VCH, Weinheim, 1998;
(c) A.D. Garnovskii, A.P. Sadimenko, M.I. Sadimenko, D.A. Garnovskii, Coord. Chem. Rev. 173 (1998) 31;
(d) G.R. Newkome, Chem. Rev. 93 (1993) 2067.
[5] L. Mahalakshmi, D. Stalke, in: D.A. Atwood, H.W. Roesky, (eds.), Structure and Bonding—Group 13 Elements, Springer-Verlag, Heidelberg, 103 (2002) 85.
[6] (a) R. Wiedemann, R. Fleischer, D. Stalke, H. Werner, Organometallics 16 (1997) 866;
(b) M. Manger, J. Wolf, M. Laubender, M. Teichert, D. Stalke, H. Werner, Chem. Eur. J. 3 (1997) 1442;
(c) H. Werner, M. Manger, M. Laubender, M. Teichert, D. Stalke, J. Organomet. Chem. 569 (1998) 189;
(d) M. Manger, J. Wolf, M. Teichert, D. Stalke, H. Werner, Organometallics 17 (1998) 3210;
(e) G. Fries, J. Wolf, M. Pfeiffer, D. Stalke, H. Werner, Angew. Chem. 112 (2000) 575;
(f) G. Fries, J. Wolf, M. Pfeiffer, D. Stalke, H. Werner, Angew. Chem. Int. Ed. Engl. 39 (2000) 564;
(g) G. Fries, K. Ilg, M. Pfeiffer, D. Stalke, H. Werner, Eur. J. Inorg. Chem. (2000) 2597.
[7] T. Kottke, D. Stalke, Chem. Ber./Recl. 130 (1997) 1365.
[8] M. Pfeiffer, T. Kottke, D. Stalke, in: H. Werner, P. Schreier (Eds.), Selective Reactions of Metal-Activated Molecules, Vieweg Verlag, Braunschweig, 1998, p. 235.
[9] G. Becker, H.P. Beck, Z. Anorg. Allg. Chem. 430 (1977) 77.
[10] (a) G. Becker, M. Birkhahn, W. Massa, W. Uhl, Angew. Chem. 92 (1980) 756;
(b) G. Becker, M. Birkhahn, W. Massa, W. Uhl, Angew. Chem. Int. Ed. Engl. 19 (1980) 741.
[11] F. Lindenberg, J. Sieler, E. Hey-Hawkins, Phosphorus, Sulfur Silicon Relat. Elem. 108 (1996) 279.
[12] U. Klingebiel, M. Meyer, U. Pieper, D. Stalke, J. Organomet. Chem. 408 (1991) 19.
[13] P.B. Hitchcock, H.A. Jasmin, M.F. Lappert, H.D. Williams, J. Chem. Soc. Chem. Commun. 22 (1986) 1634.
[14] G. Becker, H.P. Beck, Z. Anorg. Allg. Chem. 430 (1977) 91.
[15] A. Steiner, D. Stalke, J. Chem. Soc. Chem. Commun. (1993) 444.
[16] A. Steiner, D. Stalke, Organometallics 14 (1995) 2422.
[17] (a) H. Gornitzka, D. Stalke, Angew. Chem. 106 (1994) 695;
(b) H. Gornitzka, D. Stalke, Angew. Chem. Int. Ed. Engl. 33 (1994) 693;
(c) H. Gornitzka, D. Stalke, Organometallics 13 (1994) 4398.
[18] H. Gornitzka, D. Stalke, Eur. J. Inorg. Chem. (1998) 311.
[19] M. Pfeiffer, PhD thesis, Universität Würzburg: Reaktivität und Koordinationsverhalten ambidenter Ligandensysteme, Logos Verlag Berlin, 2000.
[20] (a) M. Pfeiffer, F. Baier, T. Stey, D. Leusser, D. Stalke, B. Engels, D. Moigno, W. Kiefer, in: T Clark (Ed.), Highlights in Computa-

tional Chemistry, Springer-Verlag, Heidelberg, 2001 1381;
(b) M. Pfeiffer, F. Baier, T. Stey, D. Leusser, D. Stalke, B. Engels, D. Moigno, W. Kiefer, J. Mol. Model. 6 (2000) 299.
[21] M. Pfeiffer, T. Stey, H. Jehle, B. Klüpfel, W. Malisch, V. Chandrasekhar, D. Stalke, J. Chem. Soc. Chem. Commun. (2001) 337.
[22] (a) H. Staudinger, J. Meyer, Helv. Chim. Acta 2 (1919) 635;
(b) W. Buchner, W. Wolfsberger, Z. Naturforsch. Teil. B 29 (1974) 328;
(c) T.A. Albright, W.J. Freeman, E.E. Schweizer, J. Org. Chem. 41 (1976) 2716;
(d) F. Weller, H.-C. Kang, W. Massa, T. Rübenstahl, F. Kunkel, K. Dehnicke, Z. Naturforsch. Teil. B 50 (1995) 1050.
[23] A. Steiner, PhD thesis, Universität Göttingen: Aromatische N-Heterocyclen als verbrückende Substituenten zwischen höheren Hauptgruppenhomologen, Cuvillier Verlag Göttingen, 1995, 50.
[24] (a) A. Steiner, D. Stalke, Angew. Chem. 107 (1995) 1908;
(b) A. Steiner, D. Stalke, Angew. Chem. Int. Ed. Engl. 34 (1995) 1752.
[25] S. Wingerter, H. Gornitzka, R. Bertermann, S.K. Pandey, J. Rocha, D. Stalke, Organometallics 19 (2000) 3890.
[26] S. Wingerter, M. Pfeiffer, T. Stey, M. Bolboacá, W. Kiefer, V. Chandrasekhar, D. Stalke, Organometallics 20 (2001) 2730.
[27] S. Wingerter, H. Gornitzka, G. Bertrand, D. Stalke, Eur. J. Inorg. Chem. (1999) 173.
[28] S. Wingerter, PhD thesis, Universität Würzburg: Iminophosphorane und Aminoiminophosphorane—Reaktivitäten und Koordinationsverhalten, Cuvillier Verlag Göttingen, 1999.
[29] S. Wingerter, M. Pfeiffer, F. Baier, T. Stey, D. Stalke, Z. Anorg. Allg. Chem. 626 (2000) 1121.
[30] K.L. Paciorek, R.H. Kratzer, J. Org. Chem. 31 (1966) 2426.
[31] H. Schmidbaur, K. Schwirten, H. Pickel, Chem. Ber. 102 (1969) 564.
[32] (a) W. Wolfsberger, W. Hager, Z. Anorg. Allg. Chem. 425 (1976) 169;
(b) W. Wolfsberger, W. Hager, Z. Anorg. Allg. Chem. 433 (1977) 247.
[33] A. Steiner, D. Stalke, Inorg. Chem. 32 (1993) 1977.
[34] R. Fleischer, D. Stalke, Inorg. Chem. 36 (1997) 2413.
[35] S. Wingerter, M. Pfeiffer, A. Murso, C. Lustig, T. Stey, V. Chandrasekhar, D. Stalke, J. Am. Chem. Soc. 123 (2001) 1381.